An Anatomic and Kinematic Analysis of a New Total Wrist Arthroplasty Design

Alexander W. Hooke, MA[2] Kurt Pettersson, MD, PhD[1] Marcus Sagerfors, MD[1] Kai-nan An, PhD[2] Marco Rizzo, MD[3]

[1] Department of Hand Surgery, Faculty of Medicine and Health, Örebro University, Örebro, Sweden
[2] Materials and Structural Testing Core Laboratory, Mayo Clinic, Rochester, Minnesota
[3] Department of Orthopedic Surgery, Mayo Clinic, Rochester, Minnesota

Address for correspondence Marco Rizzo, MD, Department of Orthopedic Surgery, Mayo Clinic, 200 First St. SW, Rochester, MN 55905 (e-mail: Rizzo.marco@mayo.edu).

J Wrist Surg 2015;4:121–127.

Abstract

Background Total wrist arthroplasty (TWA) is a viable surgical treatment for disabling wrist arthritis. While current designs are a notable improvement from prior generations, radiographic loosening and failures remain a concern.

Purpose The purpose of this investigation is to evaluate a new total wrist arthroplasty design kinematically. The kinematic function of a native, intact cadaveric wrist was compared with that of the same wrist following TWA.

Method Six, fresh-frozen wrist cadaveric specimens were utilized. Each wrist was fixed to an experimental table and its range of motion, axis of rotation, and muscle moment arms were calculated. The following tendons were attached to the apparatus to drive motion: extensor carpi radialis longus (ECRL), extensor carpi radialis brevis (ECRB), extensor carpi ulnaris (ECU), flexor carpi radialis (FCR), flexor carpi ulnaris (FCU), and abductor pollicis longus (APL). The wrist was then manually moved along a guide by an experimenter through a series of motions including flexion-extension, radial-ulnar deviation, and circumduction. The experiment was then performed on the specimen following implantation of the TWA.

Results Following the TWA procedure, there were statistically significant decreases in the ulnar deviation and the flexion/ulnar deviation component of dart throw ranges of motion. There were no statistically significant changes in flexion, extension, radial deviation, the extension/radial deviation component of the dart thrower motion, or the circumduction range of motion.

Conclusions Kinematic analysis of the new TWA suggests that a stable, functional wrist is achievable with this design.

Clinical Relevance While appreciating the limitations of a cadaveric study, this investigation indicates that the TWA design studied merits study in human populations.

Keywords
- arthroplasty
- rheumatoid
- total wrist
- joint
- biomechanics

Introduction

Total wrist arthroplasty (TWA) is an established surgical treatment for wrist arthritis. Several generation of designs for TWA implants have been utilized over the last 40 years. Although the newest-generation designs have some notable differences, they share features of peg/screw fixation distally into the carpus and a press-fitted proximal radial component. They also have a metal-plastic articulation. Early and second-generation designs have had difficulty with long-term

DOI http://dx.doi.org/10.1055/s-0035-1549288.
ISSN 2163-3916.

efficacy and survivorship.[1,2] To date, arthrodesis remains a more commonly utilized procedure.[3] Newer-generation implants have demonstrated improved performance compared with the earlier designs and have reported encouraging early to mid-term outcomes.[4–6] However, longer-term evaluations have demonstrated problems with failures, and survivorship data have been less than encouraging.[7] This underscores the need for improvements. As a result of some of these difficulties, a new design of implant has been proposed. The implant has a press-fitted proximal component and polyether ether ketone (PEEK) articulating surface with a peg-screw fixation method distally (►**Fig. 1**). The aim of this study is to quantify the biomechanical function of this implant and compare this function to that of an intact wrist using a cadaveric model.

The authors recognize the need to validate this new implant kinematically, and the aim of this article is to investigate performance differences between normal wrist function and wrist function following implantation of the new total wrist replacement design.

Materials and Methods

Study Design

Six, fresh-frozen wrist cadaveric specimens were used (4 female, 2 male, age 80.3 ± 12.3). Each specimen consisted of the distal forearm and hand. Specimens were screened for any joint disease or previous trauma by radiographic examination.

Each specimen was fixed to the experimental table along with a specially developed jig for positioning the wrist. Muscles were neutrally preloaded based on previous studies of wrist kinematics.[8] The forearm was mounted in a neutral pronation-supination position. A pin placed through the long axis of the third metacarpal was used for guiding the wrist through passive motion (►**Fig. 2**). A load cell was mounted on the metacarpal pin perpendicular to the axis of the pin, and lever arm distance from the load cell to the wrist joint was measured. This system allowed the torque applied to the joint to be computed by multiplying the load cell's force reading by the lever arm. Range of motion (ROM) values were then taken at an objective torque value.

A series of functional tests were completed on each wrist specimen. Testing was done once on the normal wrist, prior to surgery, and once on the postoperative wrist. The surgical approach was performed from the dorsal aspect of the wrist to provide exposure and implant the prosthesis. The wrist was manually moved through its passive ROM for four independent motions: wrist flexion/extension, radial/ulnar deviation, dart thrower motion (wrist extension, radial deviation to wrist flexion with ulnar deviation), and circumduction. For the motions along a singular axis (flexion/extension, radial/ulnar deviation, and dart throw) the specimen was moved along the desired axis using the rod in the third metacarpal along an arched guide (►**Fig. 2**). In the case of circumduction, the experimenter manually guided the hand through the maximum circumduction range of motion using the rod in the third metacarpal.

Fig. 1 The new implant. It has a PEEK-metal articulation with a radial stem and peg-screw fixation distally.

Kinematic Analysis

An electromagnetic tracking system (FastTrak, Polhemus, Inc., Colchester, VT, USA) was used to collect the kinematic data with errors of less than 2°.[9] Magnetic tracking sensors were mounted to the third metacarpal and distal radius via fiberglass rods press-fitted into drilled holes. The effect of the procedure was quantified by analyzing the ROM and computing the location of the axis rotation for each motion. The ROM was taken when the torque applied to the joint was 1 Nm. Circumduction range of motion was quantified by looking at the radius of the two-dimensionally (2D) projected circular trajectory of the distal end of the third metacarpal, with a larger radius indicating a greater range of motion.

Axis of Rotation

The instantaneous helical axis of rotation was computed to quantify the rotational function of the joint. This method, developed by and Spoor and Woltring, defines a single screw-axis and its orientation in space about which the joint is moving at each instant.[10,11] These data were extracted from the electromagnetic tracking system data. The orientation of the instantaneous helical axis, as well is its piercing point with the anatomical planes, helped us to compare the functionality of the intact joint with that of the various surgical procedures. This method was validated internally to ≤1.5-mm precision.

To quantify how the instantaneous axis of rotation of the wrist was affected by the wrist implant, the piercing point metric was utilized. The piercing point quantifies changes in the axis of rotation of the wrist as it passes through a given plane.[12] Three piercing points were computed in this study:

1. The dorsal/volar (Y) position where the axis pierces the dorsal/volar (Y–Z) plane during flexion/extension
2. The proximal/distal (Z) position where the axis pierces the dorsal/volar (Y–Z) plane during flexion/extension
3. The mediolateral (X) position where the axis pierces the mediolateral (X–Z) plane.

These two metrics were studied in two different ways.

First, the mean instantaneous axis was calculated and the distance between the mean axis's piercing point and the system origin (located at the midpoint between the radial and ulnar styloids) was computed. The piercing point position

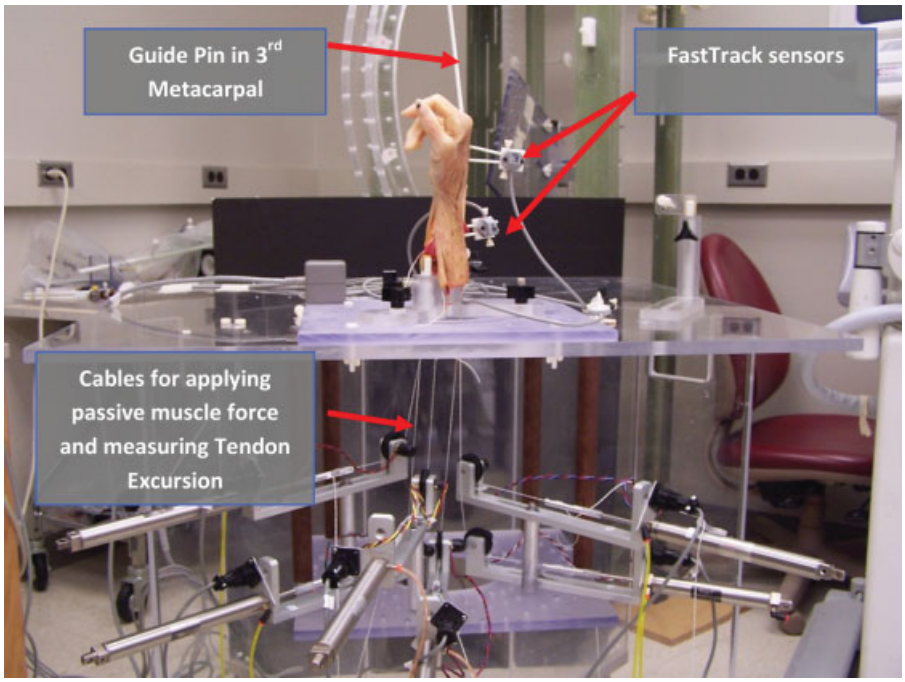

Fig. 2 Example of experimental setup. Specimen is fixed vertically to the experimental table along with custom jig for positioning the wrist. Pneumatic cylinders are used to replicate passive muscle force; rotational potentiometers are used for recording tendon excursion; a fiberglass pin is inserted in the third metacarpal for guiding the hand motion; and FastTrak sensor is used for recording kinematics.

addresses the question "How much does the wrist implant affect the axis of rotation's average position?"

Second, the standard deviation of the position of the instantaneous axis of rotation through the course of a movement cycle was computed. The piercing point variability addresses the question "How much did the piercing point shift during motion?"

Muscle Moment Arm Analysis

The moment arm of a muscle is an indicator of the efficiency of the muscle for rotating a joint about a particular axis of rotation. The muscle moment arms were measured using the tendon excursion and joint displacement method. The basic equipment for this method consisted of an electromagnetic tracking system for monitoring joint motion and electropotentiometers for monitoring tendon excursions. From the tendon displacement versus joint displacement curve, the slope at various joint angles throughout the range of joint motion was derived, which represents the moment arm about the center of rotation of that particular muscle in the plane of motion.[13,14] The effect of joint repair was quantified by analyzing changes in the muscle moment arm following surgery. These were not computed for the dart throw or circumduction motions because they require motion about a singular, anatomical axis to be quantified, and this was not an option for these conditions.

Statistical Analysis

The ROM, axis of rotation, and muscle moment arm data were analyzed using a one-way repeated measures ANOVA with post hoc comparisons performed with Tukey HSD and $p < 0.05$.

Results

Range of Motion

The ROM results comparing the intact wrist and postoperative wrist are presented in ►**Fig. 3a–d**. Following the TWA procedure, there were statistically significant decreases in the ulnar deviation and the flexion/ulnar deviation component of dart throw ranges of motion. There were no statistically significant changes in flexion, extension, radial deviation, the extension/radial deviation component of the dart throw, or circumduction range of motion. The flexion/extension, radial/ulnar deviation, and dart throw ranges of motion are presented as angles of measurement, while the circumduction range of motion is presented as the radius of the 2D projected circular trajectory of the distal end of the third metacarpal.

Axis of Rotation

The instantaneous axis of rotation, also known as the instantaneous helical axis, changes as the hand passes through its range of motion. An illustration of how this axis shifts and changes orientation throughout the range of motion is displayed in ►**Fig. 4a,b**. In this plot, a representative trial of a single specimen is shown. The trajectory of the hand is displayed with a solid blue arc, representing the intact condition. The instantaneous helical axes are displayed as the series of lines passing through the wrist region. The blue-to-green (dark-to-light) transitioning lines represent the position and orientation of the instantaneous helical axis as it moves from flexion to extension.

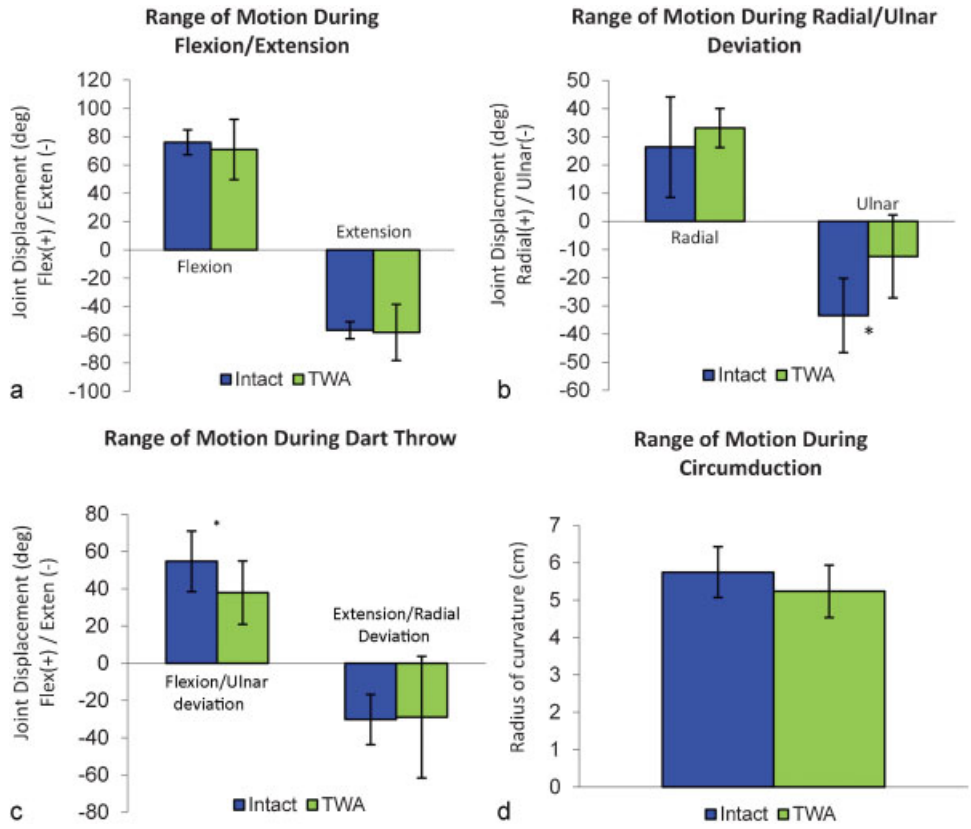

Fig. 3 The range of motion of the intact wrist and the wrist following TWA in different functional motions: (**a**) Flexion/extension. (**b**) Radial-ulnar deviation. (**c**) Dart throw motion. (**d**) Circumduction range of motion. In all cases the intact wrist is in blue and the postoperative wrist is in green. (**a–c**) present range of motion as angles in degrees; (**d**) presents the radius of the 2D projected circular trajectory of the distal end of the third metacarpal. * = significant difference at $p < 0.05$.

Mean Piercing Point Position Changes

The changes in the mean piercing point position over the course of one movement cycle are shown in ►**Fig. 5a–c**. Each line represents the shift in mean piercing point location from the intact wrist to the post-operative wrist.

►**Fig. 5a** shows the dorsal-volar shift of the mean piercing point during flexion/extension. In this figure, a positive-sloping line indicates that the mean axis of rotation shifts to a more volar position. Four specimens show a volar shift after the implantation of the wrist device, while two specimens show a dorsal shift. One specimen's volar shift was notable larger than the others, a shift of nearly 15 mm.

►**Fig. 5b** shows the distal-proximal shift of the mean piercing point during flexion-extension. In this figure, a positive-sloping line indicates that the mean axis of rotation shifts to a more distal position. All specimens showed a proximal shift in the mean piercing point position of 3–8 mm. This indicates that implantation shifts the axis of rotation of the wrist to a more proximal position.

►**Fig. 5c** shows the mediolateral shift of the piercing point during radial-ulnar deviation. In this figure, a positive-sloping line indicates that the mean axis of rotation shifts to a more radial position. Four specimens showed an ulnar shift in axis ranging in magnitude from 3 to 8 mm, one specimen showed no change, and one specimen showed a radial shift of 6 mm.

Piercing Point Variability during Movement Cycle

The variability of the piercing point over a movement cycle is shown in ►**Fig. 6a–c**. Each line represents one specimen and the change in variability of the piercing point between the intact and postoperative conditions. A positive-sloping line indicates that the piercing point had more movement in a given axis during movement cycle with the wrist implant than without the implant.

►**Fig. 6a** shows the dorsal-volar variability during a flexion-extension cycle. Four specimens showed a decrease in variability, while two specimens showed an increase. ►**Fig. 6b** shows the distal-proximal variability during a flexion-extension cycle. Five specimens showed a decrease or no change in variability, while one specimen showed an increase. ►**Fig. 6c** shows the distal-proximal variability during a radial-ulnar deviation cycle. Four specimens showed a decrease in variability, while two specimens showed an increase.

In all movements, the postoperative wrist with the implant showed a majority of specimens with a decrease in the variability of the piercing point position. This is most likely due to the perfect symmetry and congruency of the implant, which guides the joint along a trajectory with minimal variability.

Muscle Moment Arms

The muscle moment arm results from the extensor carpi radialis longus (ECRL), extensor carpi radialis brevis (ECRB), extensor carpi ulnaris (ECU), flexor carpi radialis (FCR), flexor carpi ulnaris

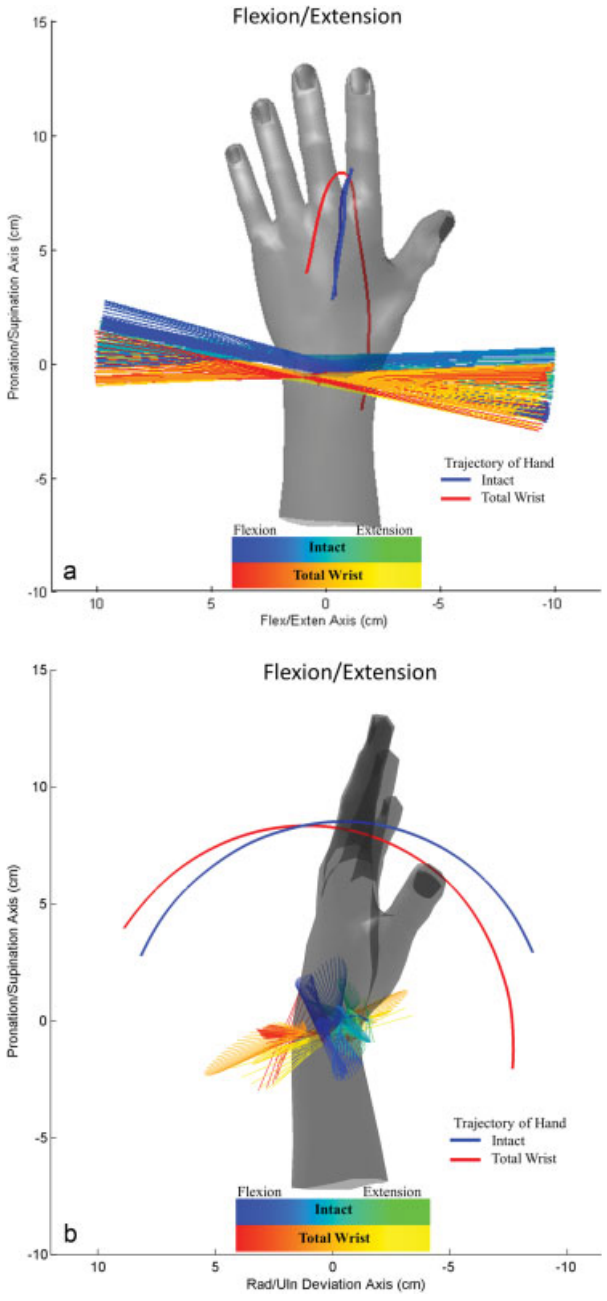

Fig. 4 Example of instantaneous helical axis computation during flexion/extension. Solid blue line = trajectory of intact hand. Solid red line = trajectory of hand with TWA. Blue/green gradient = instantaneous helical axis transition from flexion to extension. Red/yellow gradient = instantaneous helical axis transition from flexion to extension. (**a**) Dorsal view. (**b**) Lateral view.

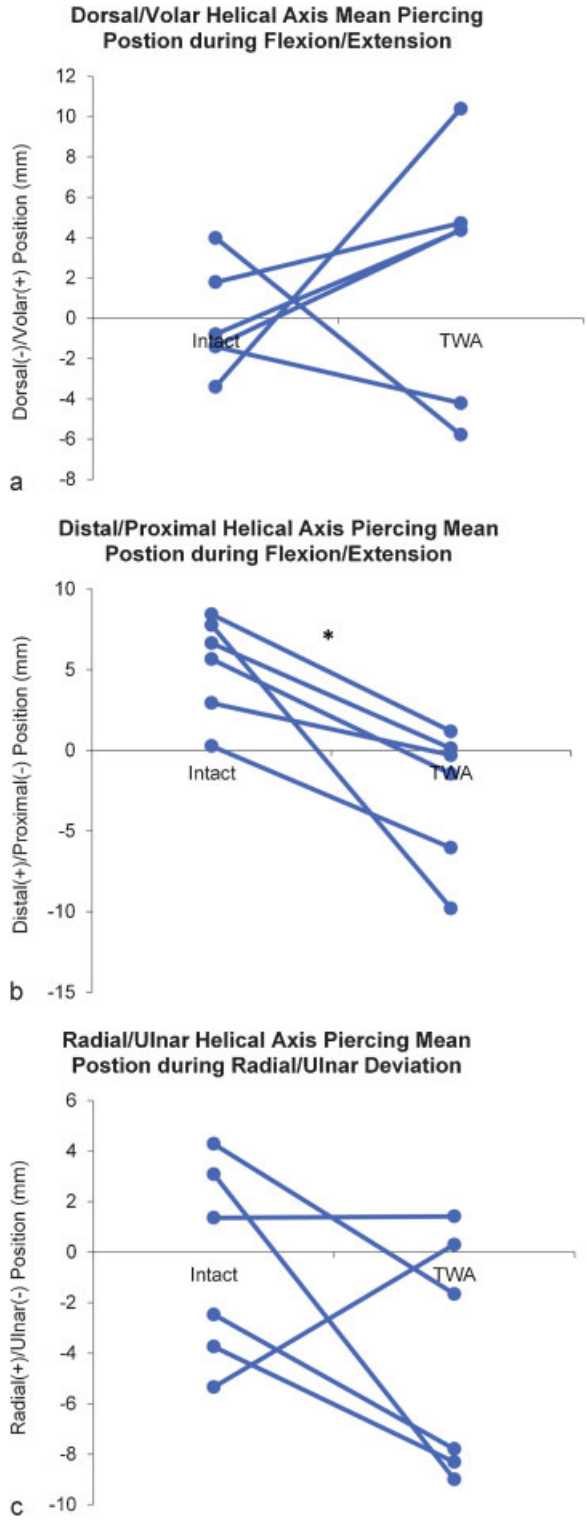

Fig. 5 The change in mean piercing point position after the TWA procedure. Each line represents one specimen. (**a**) The dorsal/volar shift during flexion-extension, with a positive-sloping line representing a volar shift. (**b**) The distal-proximal shift during flexion-extension, with a positive-sloping line representing a distal shift. (**c**) The mediolateral shift during radial-ulnar deviation, with a positive-sloping line representing a radial shift.

(FCU), and abductor pollicis longus (APL) were computed for the flexion-extension and radial-ulnar deviation tasks, and the results are shown in ►**Figs. 7** and **8**, respectively.

During flexion-extension, there was a slight change in the moment arm for the flexors and extensors. The extensor muscles ECRL, ECRB, and ECU show a slight decrease while the flexors FCR and FCU show a slight increase. None of these changes were statistically significant; however, any shortening of the extensor moment arms may result in a weakening of a patient's extension functional strength. The APL showed no change in moment arm.

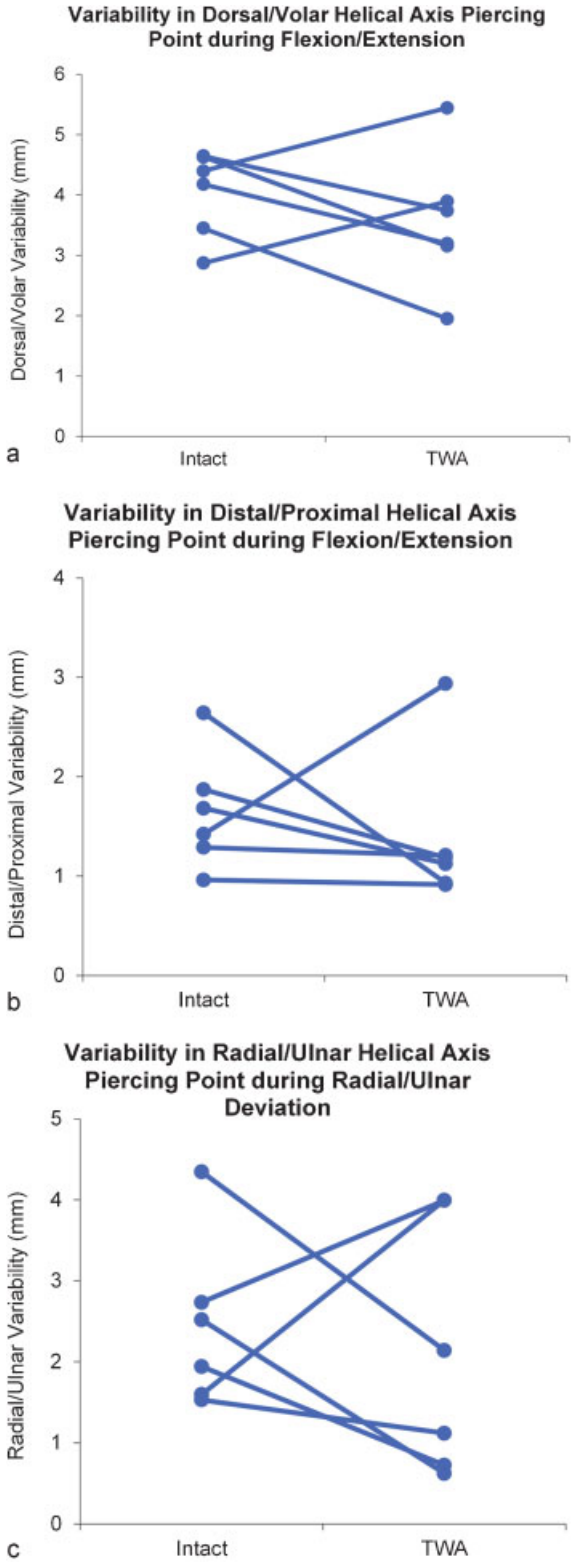

Fig. 6 Variability of the piercing point during the movement cycle. Each line represents one specimen. In all cases, a positive-sloping line indicates that the piercing point had more variation during a movement cycle with the TWA than with an intact wrist. (**a**) The dorsal-volar variability during flexion-extension. (**b**) The distal-proximal variability during flexion-extension. (**c**) The mediolateral variability during radial-ulnar deviation.

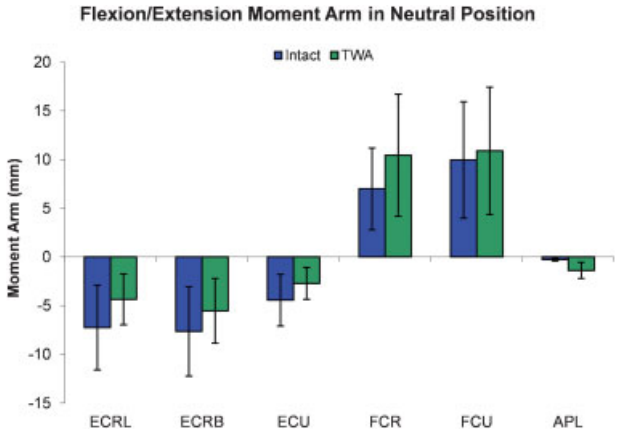

Fig. 7 Muscle moment arms in neutral position during flexion-extension for the extensor carpi radialis longus (ECRL), extensor carpi radialis brevis (ECRB), extensor carpi ulnaris (ECU), flexor carpi radialis (FCR), flexor carpi ulnaris (FCU), and abductor pollicis longus (APL) for the intact and TWA conditions.

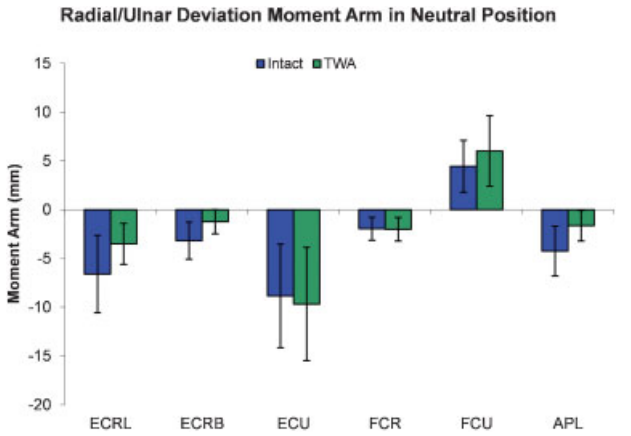

Fig. 8 Muscle moment arms in neutral position during radial-ulnar deviation for the ECRL, ECRB, ECU, FCR, FCU, and APL for the intact and TWA conditions.

During radial-ulnar deviation, there were no notable trends of changes in the muscle moment arms and no statistically significant changes. There was a large amount of variability in the moment arm values.

Discussion

The authors recognize the need to validate this new implant kinematically, and the aim of this article is to investigate performance differences between normal wrist function and wrist function following a new total wrist replacement design. Biomechanical testing of this new wrist replacement has been performed and studied extensively. The range of motion of this new TWA design showed no differences in function relative to that of the intact wrist in nearly all investigated parameters. The only motion parameters that were initially diminished compared with the native wrist were ulnar deviation and the flexion/ulnar deviation component of the dart thrower motion. Flexion, extension, and circumduction were comparable between the TWA and the native wrist.

The instantaneous axis of rotation for flexion-extension, radial-ulnar deviation, and dart-thrower motion following

wrist replacement appeared acceptable. In this study, there was a slight volar and proximal shift in the flexion-extension axis after the implantation of the wrist device. Additionally, a majority of the postimplantation wrists had a slight ulnar shift in the radioulnar axis of rotation. Regarding the variability of the axis of rotation's position within a functional motion, a majority of the postoperative wrists demonstrated a decrease in the variability of the piercing point position. This is expected because of the perfect congruency of the implant, but it also confirms that the implant's geometry will not adversely affect the wrist joint stability. All of these changes in the axis of rotation's position appear to be within an acceptable amount of deviation from the normal wrist function.

There were slight changes in the moment arm for the flexors and extensors, but none of these changes were statistically significant. This was shown to be the case with both flexion and extension as well as radial and ulnar deviation.

Surgical placement of the total wrist appeared reliably reproducible, and fluoroscopy confirmed satisfactory and consistent position in the wrist. The technique has been refined with the use of this study to help optimize the ease and safety of implantation.

Although this study is limited to the biomechanics of this implant, the outcomes from this analysis suggest that the tested implant will have similar biomechanical function to a native wrist and that use of this implant in patients would be appropriate.

Study Performed at
Mayo Clinic, Materials and Structural Testing Core Laboratory, 200 First St SW, Guggenheim 1–28, Rochester, MN 55905.

Ethical Approval
Mayo Clinic IRB ethical review committee approval: #12–008426.

Conflict of Interest
This study was funded by TriMed, Inc.

References

1 Takwale VJ, Nuttall D, Trail IA, Stanley JK. Biaxial total wrist replacement in patients with rheumatoid arthritis. Clinical review, survivorship and radiological analysis. J Bone Joint Surg Br 2002; 84(5):692–699
2 Dennis DA, Ferlic DC, Clayton ML. Volz total wrist arthroplasty in rheumatoid arthritis: a long-term review. J Hand Surg Am 1986; 11(4):483–490
3 Trail IA, Stanley JK. Total wrist arthroplasty. In: Gelberman RH, ed. The Wrist. Philadelphia, PA: Lippincott Williams & Wilkins; 2010: 457–471
4 Cooney W, Manuel J, Froelich J, Rizzo M. Total wrist replacement: a retrospective comparative study. J Wrist Surg 2012; 1(2):165–172
5 Herzberg G, Boeckstyns M, Sorensen AI, et al. "Remotion" total wrist arthroplasty: preliminary results of a prospective international multicenter study of 215 cases. J Wrist Surg 2012;1(1): 17–22
6 Ferreres A, Lluch A, Del Valle M. Universal total wrist arthroplasty: midterm follow-up study. J Hand Surg Am 2011;36(6): 967–973
7 Ward CM, Kuhl T, Adams BD. Five to ten-year outcomes of the Universal total wrist arthroplasty in patients with rheumatoid arthritis. J Bone Joint Surg Am 2011;93(10):914–919
8 Ishikawa J, Cooney WP III, Niebur G, An KN, Minami A, Kaneda K. The effects of wrist distraction on carpal kinematics. J Hand Surg Am 1999;24(1):113–120
9 Ishikawa J, Niebur GL, Uchiyama S, et al. Feasibility of using a magnetic tracking device for measuring carpal kinematics. J Biomech 1997;30(11-12):1183–1186
10 Spoor CW, Veldpaus FE. Rigid body motion calculated from spatial co-ordinates of markers. J Biomech 1980;13(4): 391–393
11 Woltring HJ. Estimation of the trajectory of the instantaneous centre of rotation in planar biokinematics. J Biomech 1990;23(12): 1273–1274
12 de Lange A. A Kinematical Study of the Human Wrist Joint [thesis]. Nijmegen, The Netherlands: University of Nijmegen; 1987
13 An KN, Takahashi K, Harrigan TP, Chao EY. Determination of muscle orientations and moment arms. J Biomech Eng 1984;106(3): 280–282
14 An KN, Ueba Y, Chao EY, Cooney WP, Linscheid RL. Tendon excursion and moment arm of index finger muscles. J Biomech 1983;16(6):419–425